PHOTOCHEMISTRY OF 3,4,9,10-PERYLENETETRACARBOXYLIC DIANHYDRIDE DYES: VISIBLE ABSORPTION AND FLUORESCENCE OF THE DI(GLYCYL)IMIDE DERIVATIVE MONOMER AND DIMER IN BASIC AQUEOUS SOLUTIONS

WILLIAM E. FORD

Radiation Laboratory, University of Notre Dame, Notre Dame, IN 46556 (U.S.A.)

Summary

The synthesis of the di(glycyl)imide derivative of 3,4,9,10-perylene-tetracarboxylic dianhydride and its spectral properties in basic aqueous solutions are described. The monomer and dimer forms of the dye coexist in H_2O (10^{-3} M NaOH) with an equilibrium association constant $K = 1.0 \times 10^7$ M^{-1} (24 °C) for dye concentrations up to 2.4×10^{-5} M (degree of dimerization equal to 96%). The 0–0 absorption band of the monomer at 532 nm is split by exciton interaction in the dimer into a higher energy band at about 500 nm and a lower energy band at about 542 nm. The fluorescence quantum yield Φ_F of the monomer is about 1.0, while the dimer is non-fluorescent ($\Phi_F < 0.02$). The addition of ethanol favors dissociation of the dimer, while the addition of NaCl favors its formation. The dye in 50vol.%-ethanol–50vol.%H_2O (10^{-3} M NaOH) has a Φ_F of 0.96 ± 0.04.

1. Introduction

The dyes derived from 3,4,9,10-perylenetetracarboxylic dianhydride have been known for several decades as vat dyes possessing excellent light fastness [1 - 3], but only recently has it been recognized that the photo-chemical stabilities of the dyes are retained in the solution phase and that the fluorescence quantum yields are high [4 - 8]. These properties make the perylene dyes attractive as potential laser dyes and photosensitizers [8]. The development of stable, efficient and inexpensive photosensitizers is crucial to the design of practical artificial photosynthetic devices as a means of converting solar energy to a stable chemical form (fuel) [9 - 12]. Colloidal aqueous solutions such as detergent micelles and lipid bilayer vesicles are currently being explored as prototypes of artificial photosynthetic systems [13 - 21]. This paper is part of an ongoing study [22] of the photo-chemical properties of imide derivatives of 3,4,9,10-perylenetetracarboxylic dianhydride in colloidal aqueous media. The solubilities of these dyes can be

controlled by varying the nature of the amine from which they are derived upon condensation between the amine and 3,4,9,10-perylenetetracarboxylic dianhydride. The mono(n-octyl)imide derivative is readily incorporated into aqueous micellar solutions, but its solubility and absorption and fluorescence properties are sensitive to pH effects, which affect the degree of protonation and hydration of the anhydride end of the molecule [22]. This sensitivity complicates the study of the photochemistry of the dye in aqueous solutions since several forms of the dye may coexist. Diimide derivatives such as the one described below are not intrinsically subject to such pH effects because both ends of the chromophore have the stable imide bond.

This report describes the synthesis and spectral properties of the di(glycyl)imide derivative of 3,4,9,10-perylenetetracarboxylic dianhydride, whose structure is shown in Fig. 1. The dye is easily synthesized in quantitative yield from the dianhydride and the potassium salt of glycine. It is readily soluble in water. Langhals et al. [5, 7] have prepared other water-soluble diimide derivatives. Although the polar groups on the di(glycyl)imide dye are located on opposite ends of the molecule (Fig. 1), the dye is amphiphilic because the polar ends are separated by a non-polar aromatic hydrocarbon region. Molecules such as this, like the water-soluble porphyrins and phthalocyanines, can bind to micelles and vesicles as a result of favorable electrostatic and van der Waals interactions [10, 19, 23 - 30]. The present study investigates the spectral properties of the di(glycyl)imide dye in basic aqueous solutions in the absence of micelles or vesicles. It is shown that the dye dimerizes, and the monomer–dimer equilibrium and spectral properties of both species are described. The physicochemical and photophysical properties of dye aggregates are the subjects of considerable theoretical and practical interest [31 - 64].
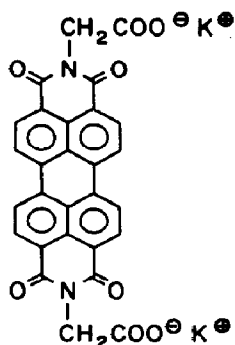

Fig. 1. Structural formula of the di(glycyl)imide (dipotassium salt) derivative of 3,4,9,10-perylenetetracarboxylic dianhydride.

2. Experimental details

2.1. Materials

Glycine (purity, better than 99%, from Fluka), 3,4,9,10-perylenetetracarboxylic dianhydride (from Aldrich) and rhodamine 6G chloride

(rhodamine 590, from Exciton) were used as received. Hexadecyltrimethyl-ammonium bromide (from Eastman) was recrystallized from ethyl acetate–EtOH (EtOH ≡ ethanol). Water was treated with a Millipore–Milli-Q purification system. All other chemical reagents and solvents were of the highest purity commercially available. Elemental analyses were performed by Schwarzkopf Microanalytical Laboratory (Woodside, NY).

The dipotassium salt of the di(glycyl)imide derivative of 3,4,9,10-perylenetetracarboxylic dianhydride (Fig. 1) was prepared in the following manner. 3,4,9,10-Perylenetetracarboxylic dianhydride (0.512 g, 1.31 mmol) was suspended in dimethyl sulfoxide (50 ml), and the suspension was heated to 100 °C with magnetic stirring in a 250 ml round-bottomed flask. A solution of glycine (2.39 g, 31.8 mmol) and 89% KOH (2.01 g, 31.8 mmol) in water (25 ml) was added dropwise to the suspension, the flask was fitted with a reflux condenser, and the mixture was stirred at 100 °C for 3 h. The resultant suspension was cooled to room temperature and the precipitate was collected by vacuum filtration, washed two times with 67vol.%(dimethyl sulfoxide)–33vol.%H_2O and three times with methanol, and dried. The yield of the dipotassium salt was 0.760 g (100% based on 3,4,9,10-perylenetetracarboxylic dianhydride). The salt was stored in a desiccator because of its slightly hygroscopic nature. The diacid form of the dye was obtained by suspending the dipotassium salt in hot aqueous 0.5 M HCl solution for 5 min. The resultant solid was washed three times with water and dried. Elemental analysis of the dipotassium salt gave the following results. Calculated for $C_{28}H_{12}N_2O_8K_2$ (molecular weight, 580.60): C, 57.72%; H, 2.08%; N, 4.81%; K, 13.42%. Found: C, 54.57%; H, 1.83%; N, 4.36%; K, 13.42%. The following absorption spectra (λ_{max} (nm) (ϵ (M^{-1} cm^{-1})) were obtained. In H_2SO_4: 558 (42 500), 593 (56 400 ± 4000). In 50vol.%EtOH–50vol.%H_2O (10^{-3} M NaOH): 491 (46 400), 527 (73 000 ± 1000). Elemental analysis of the diacid gave the following results. Calculated for $C_{28}H_{14}N_2O_8$ (molecular weight, 506.41): C, 66.40%; H, 2.79%; N, 5.53%. Found: C, 66.42%; H, 2.90%; N, 5.34%. The following absorption spectra were obtained. In H_2SO_4: 558 (43 100), 593 (57 000 ± 5000). In 50vol.%EtOH–50vol.%H_2O (10^{-3} M NaOH): 491 (48 800), 527 (76 800 ± 1000).

Although the elemental analysis of the dipotassium salt was not as expected, several observations indicate that the product was pure. (1) The elemental analysis of the diacid form of the dye, which was obtained from the dipotassium salt, was consistent with its formula, and the absorption spectra of the two forms of the dye were nearly the same in two solvent systems. (2) The synthetic yield of the dipotassium salt was exactly (100% ± 1%) as expected for complete conversion. (3) The absorption spectrum of the dipotassium salt in aqueous micellar solutions of hexadecyltrimethyl-ammonium bromide was independent of pH in the range 3 (10^{-3} M $NaHSO_4$) to 11 (10^{-3} M NaOH), which would not have been the case if the product contained either the starting dianhydride or its mono(glycyl)imide derivative as impurities. (4) The potassium analysis (atomic absorption) was as expected. These results indicate that the dipotassium salt was incompletely

combusted during the microanalysis of its carbon, hydrogen and nitrogen contents, leading to their lower than expected values.

2.2. Methods

Unless otherwise noted, all measurements were carried out at ambient temperature (24 ± 1 °C) and the solutions were saturated with air. Solutions containing the di(glycyl)imide dye for absorption and fluorescence measurements were prepared by diluting stock solutions of the dipotassium salt in water ((2.5×10^{-4}) - (1.3×10^{-3} M)) with the appropriate solvent. Absorption spectra were recorded on a Cary 219 spectrophotometer using quartz cuvettes whose path lengths (in centimeters) were either 9.93 (± 0.01), 1.000, 0.200, 0.100 or 0.0105 (± 0.0005). All values of ϵ that are reported below were based on the value of 76 800 M^{-1} cm^{-1} at 527 nm in 50vol.%EtOH–50vol.%H$_2$O (10^{-3} M NaOH). Oscillator strengths OS of the visible wavelength transition were calculated according to the equation [32, 39, 65, 66]

$$OS = 4.32 \times 10^{-9} \int \epsilon(\tilde{\nu}) \, d\tilde{\nu}$$

where the integral was obtained from absorption spectra using a planimeter. It should be noted that the oscillator strength is sometimes calculated by multiplying the above expression for OS by a constant that includes the refractive index of the solvent [35, 66 - 68].

Corrected fluorescence emission and excitation spectra were obtained using an SLM 8000 photon-counting spectrofluorometer. The excitation and detection were at right angles to one another using 1.0 cm square quartz cuvettes. The excitation and emission bandpasses ranged from 2 to 8 nm, depending on the concentration of dye. The spectra were measured in the ratio mode using a solution of rhodamine B perchlorate in ethylene glycol (5.7 g l^{-1}) as the quantum counter. The fluorescence quantum yield of the di(glycyl)imide dye in 50vol.%EtOH–50vol.%H$_2$O (10^{-3} M NaOH) was measured using the optically dilute relative method using rhodamine 6G in absolute EtOH ($\Phi_F = 0.95$) as the standard [69]. The yields of solutions of the dye in H$_2$O (10^{-3} M NaOH) were measured relative to solutions containing equimolar concentrations of the dye in 50vol.%EtOH–50vol.%H$_2$O (10^{-3} M NaOH). The excitation wavelengths for these measurements were 472 and 508 nm, and the excitation and emission bandpasses used were the same for both the sample and the reference solutions. The quantum yields determined for the two excitation wavelengths were averaged. There was no evidence of photodecomposition of the dye during these measurements. Other details of the instrumentation and quantum yield determinations are available in a previous publication [22].

3. Results

Visible absorption spectra of solutions of the di(glycyl)imide dye in H$_2$O containing 10^{-3} M NaOH in the concentration range (8.7×10^{-9}) -
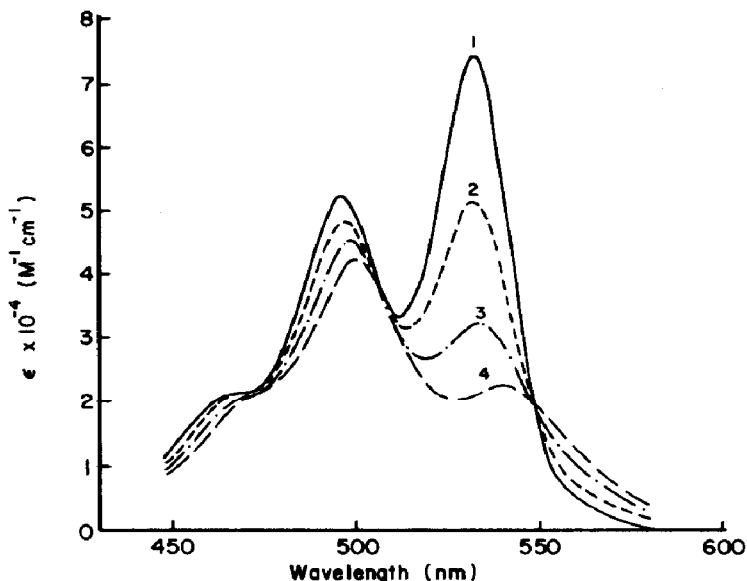
Fig. 2. Visible absorption spectra of solutions of the di(glycyl)imide dye in H_2O (10^{-3} M NaOH) (24 °C). Curve 1: concentration, 8.7×10^{-9} M; path length, 9.93 cm. Curve 2: concentration, 1.1×10^{-7} M; path length, 9.93 cm. Curve 3: concentration, 8.2×10^{-7} M; path length, 9.93 cm. Curve 4: concentration, 2.4×10^{-5} M; path length, 1.00 cm.

(2.4×10^{-5}) M are shown in Fig. 2. Increasing the concentration of dye caused the spectrum to change from one with maxima near 495 and 532 nm to one with maxima near 500 and 542 nm, with isosbestic points near 472, 508 and 548 nm. The absorption spectra broadened as the concentration was increased above 2.4×10^{-5} M up to 1.3×10^{-3} M, so that the isosbestic points were lost. In contrast, the absorption spectrum of the dye in 50vol.%-EtOH−50vol.%H_2O containing 10^{-3} M NaOH was independent of concentration in the range (3×10^{-7}) - (1×10^{-5}) M. The fluorescence excitation and emission spectra of the dye in the two solvent systems were similar, with the band maxima shifted by 5 - 10 nm to higher wavelengths in the purely aqueous solvent (Fig. 3). The excitation spectrum of the dye in the EtOH−H_2O solvent closely resembled its absorption spectrum (not shown). The fluorescence quantum yield of the dye in this solvent was 0.96 ± 0.04, and the spectral properties are summarized in Table 1. These characteristics are typical of the diimide derivatives of 3,4,9,10-perylenetetracarboxylic dianhydride [4 - 6, 22].

The spectral changes shown in Fig. 2 indicated that the dye monomer and an aggregated form of the dye coexisted in H_2O (10^{-3} M NaOH). The presence of isosbestic points indicated that only the monomer and an n-mer were involved. The aggregation of dyes in aqueous media generally involves the dimer as an intermediate to higher aggregates. The monomer−dimer (M−D) equilibrium is characterized by the equilibrium constant

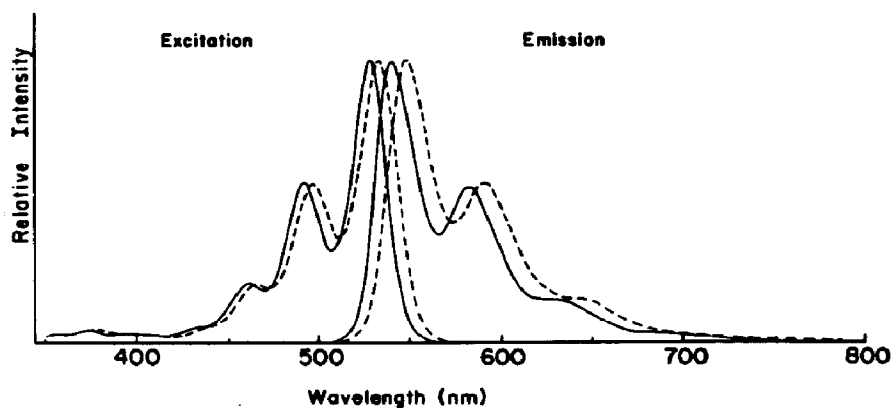$$K = \frac{[D]}{[M]^2} \qquad (M + M \rightleftharpoons D) \qquad (1)$$

Fig. 3. Normalized fluorescence excitation and emission spectra of solutions of the di(glycyl)imide dye (24 °C): ——, in 50vol.%EtOH–50vol.%H$_2$O containing 10^{-3} M NaOH; – – –, in H$_2$O containing 10^{-3} M NaOH.

TABLE 1

Visible absorption and fluorescence excitation and emission spectral data and fluorescence quantum yields of the di(glycyl)imide derivative of 3,4,9,10-perylenetetracarboxylic dianhydride[a, b]

Solvent[c]	Absorption			Excitation		Emission		
	λ_1	λ_2	$\epsilon \times 10^{-4}$	λ_1	λ_2	λ_1	λ_2	Φ_F
50vol.%EtOH–	491	527	7.7	492	528	540	583	0.96
50vol.%H$_2$O	0.64	1.00		0.56	1.00	1.00	0.55	
H$_2$O	496	532	8.4	497	533	547	592	1.14
(monomer)[d]	0.64	1.00		0.56	1.00	1.00	0.56	
H$_2$O (dimer)[d]	500	542	4.2	—	—	—	—	< 0.02
	1.00	0.51						

[a]Conditions: air-saturated solutions; $T = 24 \pm 1$ °C.
[b]Spectral characteristics: the λ (nm) are the peak positions of the two most intense bands whose relative intensities are listed underneath these values. The ϵ (M^{-1} cm^{-1}) is the molar extinction coefficient of the most intense absorption band. The spectral resolution is ± 1 nm for absorption, ± 2 nm for excitation and ± 1 nm for emission. The estimated uncertainties in the values of ϵ and Φ_F are ± 5% in EtOH–H$_2$O and ± 10% in H$_2$O.
[c]All solutions contained 10^{-3} M NaOH.
[d]The absorption spectral properties and Φ_F of the monomer and dimer were obtained by extrapolation (see text).

The material balance in the equation

$$c = [M] + 2[D] \tag{2}$$

relates the concentration of monomer and dimer to the overall concentration c of dye. The fraction

$$f_M = \frac{[M]}{c} \tag{3}$$

of dye present as monomer approaches the limiting values of 1 and 0 as c decreases and increases respectively. The concentration dependence of the spectral changes that are exemplified in Fig. 2 was tested for compliance to eqns. (1) - (3) using the graphical approach attributed to Scheibe [31, 33, 35, 37]. It follows from the definitions of K, c and f_M (eqns. (1) - (3)) that a plot of the logarithm of the concentration of dye present as dimer $((1 - f_M)c)$ vs. the logarithm of the concentration present as monomer $(f_M c)$ is linear with a slope of $n = 2$:

$$\log(1 - f_M)c = \log K + \log n + n \log(f_M c) \tag{4}$$

In order to use eqn. (4), some knowledge of the spectral properties of the pure monomer and dimer species is required. Figure 4 shows a plot of the ratio of the extinction coefficient of the dye at 532 nm to that at 508 nm ($\epsilon_{532}/\epsilon_{508}$) as a function of $\log c$. This ratio was selected because the change in ϵ for the conversion of monomer to dimer was maximal near 532 nm (Fig. 2); division of ϵ_{532} by the isosbestic value of ϵ_{508} $((3.53 \pm 0.15) \times 10^4 \ M^{-1} \ cm^{-1})$ reduced the effects of uncertainties in the absolute values of ϵ_{532} owing to non-systematic errors in the values of c of the samples. This ratio should be related to f_M according to the equation
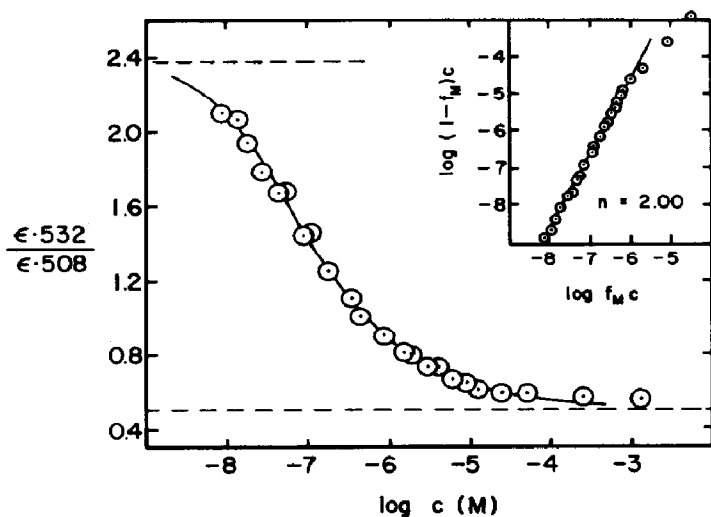

Fig. 4. Ratio of ϵ_{532} to ϵ_{508} as a function of the logarithm of concentration of the di(glycyl)imide dye in H_2O $(10^{-3}$ M NaOH) (24 °C). The full curve was calculated according to eqns. (4) and (5) with $K = 1.03 \times 10^7 \ M^{-1}$, $n = 2.00$ and the limiting values of $\epsilon_{532}/\epsilon_{508}$ indicated by the broken lines. Inset: log–log plot of the data according to eqn. (4). The slope of the straight line is $n = 2.00$.

$$f_M = \frac{(\epsilon_{532}/\epsilon_{508})_{max} - \epsilon_{532}/\epsilon_{508}}{(\epsilon_{532}/\epsilon_{508})_{max} - (\epsilon_{532}/\epsilon_{508})_{min}} \tag{5}$$

where the maximal and minimal values of $\epsilon_{532}/\epsilon_{508}$ are the values for pure monomer ($f_M = 1$) and pure dimer ($f_M = 0$) respectively. Based on the plot of experimental values of $\epsilon_{532}/\epsilon_{508}$ vs. $\log c$ in Fig. 4 and the expected sigmoidal dependence, the limiting values of $(\epsilon_{532}/\epsilon_{508})_{max} \approx 2.4$ and $(\epsilon_{532}/\epsilon_{508})_{min} \approx 0.5$ were obtained. These values were varied slightly in order to optimize the least-squares fit of the experimental points to eqn. (4). The log–log plot shown in the inset of Fig. 4 was obtained using 2.38 as the maximal value of $\epsilon_{532}/\epsilon_{508}$ and 0.51 as the minimal value. Disregarding the three points for the highest values of c in this plot, the experimental points fit eqn. (4) with a correlation coefficient of 0.9991 and a slope of 2.00. Thus, the data conformed well to the monomer–dimer equilibrium ($n = 2$) (eqn. (1)) in the concentration range $c = (8.7 \times 10^{-9}) - (2.4 \times 10^{-5})$ M. On the basis of the least-squares correlation coefficient, the maximal and minimal values of $\epsilon_{532}/\epsilon_{508}$ could be varied by ± 0.01 without a significant loss in the quality of the fit. The value of the equilibrium constant K, which was determined from the slope and the intercept of the log–log plot (eqn. (4)), equaled $(1.03 \pm 0.03) \times 10^7$ M^{-1}. The theoretical curve (full line) drawn in the plot of $\epsilon_{532}/\epsilon_{508}$ vs. $\log c$ (Fig. 4) fit the experimental points well in the concentration range $c = (8.7 \times 10^{-9}) - (2.4 \times 10^{-5})$ M, over which the fraction f_M of dye present as monomer ranged from 0.84 to 0.04.

The visible absorption spectra of the pure monomer and dimer were extrapolated from the experimental spectra by an iterative calculation. The two spectra used in this calculation were the ones shown in Fig. 2 with $c = 8.7 \times 10^{-9}$ M ($f_M = 0.84$) and $c = 2.4 \times 10^{-5}$ M ($f_M = 0.04$). It was assumed that the extinction coefficients of these samples at any wavelength were the weighted-average values of the extinction coefficients of the pure monomer (ϵ_M) and dimer ($\epsilon_D/2$) at that wavelength:

$$\epsilon = f_M \epsilon_M + \frac{(1 - f_M)\epsilon_D}{2} \tag{6}$$

In the first iteration, ϵ_M was calculated from the spectrum with $f_M = 0.84$ by using the spectrum with $f_M = 0.04$ as an approximation for $\epsilon_D/2$. This value of ϵ_M was then used to calculate $\epsilon_D/2$ from the spectrum with $f_M = 0.04$. Two more iterations were used to calculate ϵ_M and $\epsilon_D/2$. The values of ϵ_M and $\epsilon_D/2$ obtained from the third iteration were the same as those from the second iteration, so these values were assumed to be the correct ones. The spectra of the monomer and dimer in H_2O (10^{-3} M NaOH) are shown in Fig. 5 and summarized in Table 1. The oscillator strength of the visible transition of the monomer was 0.75 ± 0.02 and that of the dimer was 0.50 ± 0.01 (per monomer component).

The fluorescence excitation and emission spectra of the di(glycyl)imide dye in H_2O (10^{-3} M NaOH) that are shown in Fig. 3 were obtained with a dye concentration of 3.5×10^{-7} M. At this concentration, about two-thirds
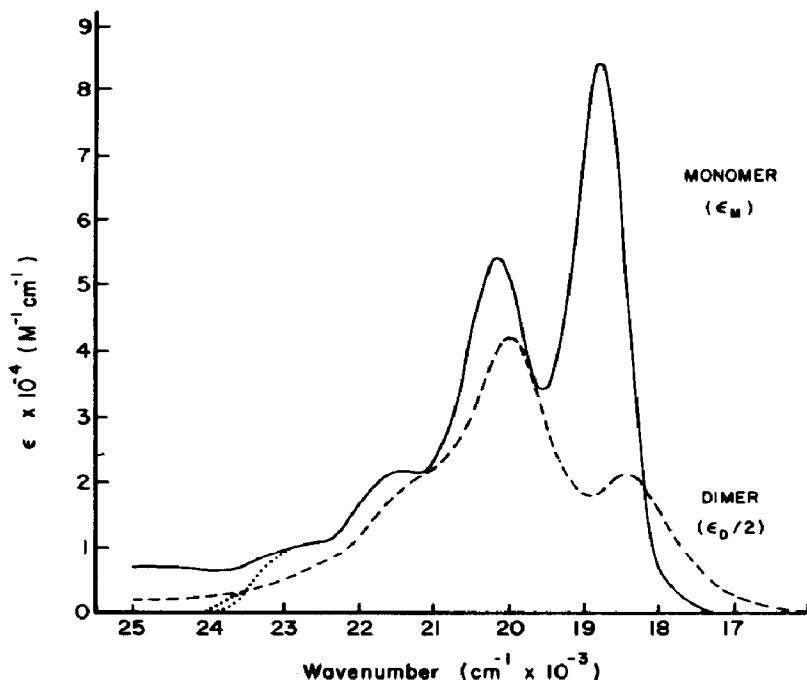
Fig. 5. Extrapolated visible absorption spectra of the monomer (———) and dimer (- - - -) forms of the di(glycyl)imide dye in H_2O (10^{-3} M NaOH). The extinction coefficient of the dimer is per monomer component. The dotted lines show the high wavenumber limits of the spectra used in calculating oscillator strengths. The extinction coefficient of the monomer may be too high for wavenumbers above 23 000 cm^{-1} owing to baseline uncertainties.

of the dye was present as the dimer. The parallellism between the spectra in H_2O and those in $EtOH-H_2O$ (Fig. 3) and the similarity between the excitation spectrum in H_2O to the extrapolated absorption spectrum of the monomer (Fig. 5) indicated that only the dye monomer was fluorescent. Excitation and emission spectra obtained at dye concentrations of 10^{-3} M using front-face excitation were also entirely attributable to the monomer, although they were distorted by self-absorption effects. The non-fluorescent nature of the dimer was further supported by the quantum yield measurements described below. The band maxima and relative intensities of the excitation and emission spectra of the monomer in H_2O (10^{-3} M NaOH) are summarized in Table 1.

Evidence for fluorescence from aggregates of the di(glycyl)imide dye was obtained using a solution of the dye (2.4×10^{-6} M) in saturated aqueous lithium acetate containing 10^{-3} M NaOH, which formed a clear glass when frozen with liquid nitrogen (77 K). The visible absorption spectrum of the solution at room temperature (24 °C) was broad with maxima near 475 nm ($\epsilon = 20\,300$ M^{-1} cm^{-1}), 505 nm (19 600 M^{-1} cm^{-1}) and 560 nm (14 200 M^{-1} cm^{-1}). This spectrum had the three-banded character of the dimer spectrum (Fig. 5), but the extinction coefficients (per monomer component) were reduced, the bands were red shifted and broadened considerably and the

relative intensities of the maxima were shifted in favor of the highest energy band near 475 nm. These differences were indicative of the presence of aggregates higher than dimers [51, 55]. The frozen sample (77 K) had a relatively weak emission with a maximum near 685 nm which was absent at room temperature. The excitation spectrum for this emission paralleled the absorption spectrum obtained at room temperature, so that its identification as an emission from the dye aggregate was unambiguous. The emission can be tentatively identified as being fluorescence because the energy gap between the singlet S_1 and triplet T_1 states of perylene, and presumably its diimide derivatives as well, is about $10\,400$ cm^{-1} [67], so that phosphorescence would be expected to occur at a wavelength much longer than 685 nm (beyond the range of the instrument used in this experiment).

The fluorescence quantum yield Φ_F of the di(glycyl)imide dye in H_2O (10^{-3} M NaOH) was measured for dye concentrations in the range (4.9×10^{-10}) - (2.8×10^{-6}) M. Figure 6 shows a plot of Φ_F as a function of $\log c$. This data was analyzed similarly to the absorption spectral data (Fig. 4). The inset in Fig. 6 shows the log–log plot according to eqn. (4) that was obtained using the limiting values of Φ_F of 1.14 ($f_M = 1$) and 0 ($f_M = 0$), where f_M was calculated according to the equation

$$f_M = \frac{\Phi_F{}^{max} - \Phi_F}{\Phi_F{}^{max} - \Phi_F{}^{min}} \tag{7}$$

instead of eqn. (5). The log–log plot of the data was linear (correlation coefficient, 0.9995), but the slope of the line was $n = 1.68$ instead of the value of
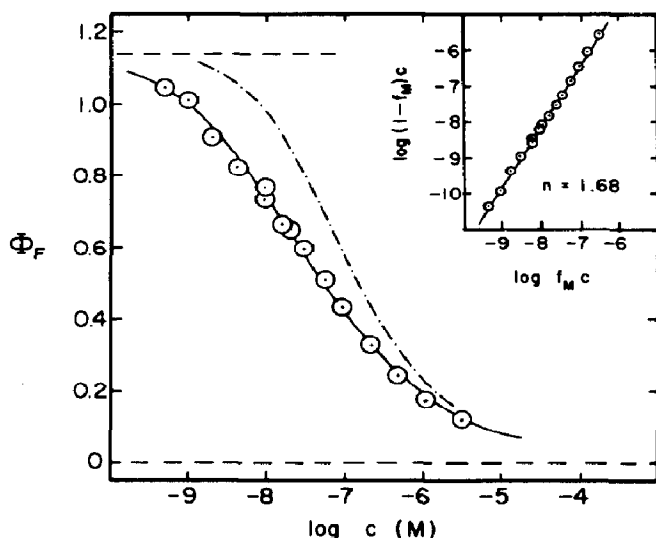

Fig. 6. Fluorescence quantum yields as a function of the logarithm of concentration of the di(glycyl)imide dye in H_2O (10^{-3} M NaOH) (24 °C). The full curve was calculated according to eqns. (4) and (7) with $K = 1.39 \times 10^5$ (non-integer units), $n = 1.68$ and the limiting values of Φ_F indicated by the broken lines. The dash-dotted curve was calculated with $K = 1.03 \times 10^7$ M^{-1} and $n = 2.00$. Inset: log–log plot of the data according to eqn. (4). The slope of the straight line is $n = 1.68$.

2.00 that was obtained from the absorption spectral data. The value of K calculated from the slope and intercept of the log–log plot was 1.39×10^5 (non-integer units). Using this value of K and $n = 1.68$, the full curve shown in the plot of Φ_F vs. log c (Fig. 6) was calculated according to eqns. (4) and (7). For comparison, the curve that is calculated with $K = 1.03 \times 10^7 \, M^{-1}$ and $n = 2.00$ is also shown in Fig. 6. The values of Φ_F for the pure monomer (Φ_F^{max}) and pure dimer (Φ_F^{min}) used in fitting the data to eqns. (4) and (7) could be varied by ± 0.01 without a significant loss in the quality of the fit. The uncertainty in the *absolute* value of Φ_F for the monomer was greater than ± 0.01, however, because it was subject to uncertainties in the absolute value of Φ_F of the dye in the reference solution as well as uncertainties in the relative optical densities of the sample and reference solutions at 472 and 508 nm. Taking these factors into account, the estimated uncertainty in the value of Φ_F^{max} was about $\pm 10\%$. Thus, it is reasonable to conclude that the fluorescence quantum yield of the monomer in H_2O (10^{-3} M NaOH) was approximately 1.0 and that of the dimer was less than 0.02.

The effect of added salt (NaCl) on the monomer–dimer equilibrium in H_2O (10^{-3} M NaOH) was examined in solutions containing 9.4×10^{-8} M of the di(glycyl)imide dye. The addition of NaCl favored dimer formation, with the fraction f_M of dye present as monomer decreasing from 0.52 (no NaCl) to 0.12 (4.0 M NaCl), as shown in Fig. 7. The values of f_M for NaCl concentrations above 0.1 M, which were calculated from eqn. (5) assuming dimer formation only, are approximate values owing to some broadening of the absorption bands that is indicative of the formation of higher aggregates (see above).
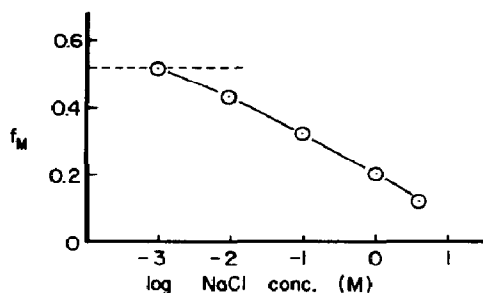

Fig. 7. Fraction of the di(glycyl)imide dye present as monomer as a function of the logarithm of NaCl concentration in H_2O (10^{-3} M NaOH) (24 °C). The dye concentration is 9.4×10^{-8} M. The broken line shows the limiting value of f_M obtained in solutions without NaCl. The full curve is intended to show the trend of the data and has no theoretical basis.

4. Discussion

The visible absorption and fluorescence properties of the di(glycyl)-imide dye in basic aqueous ethanol resemble those of other di(alkyl)imide

and di(aryl)imide dyes in organic solvents [4 - 8, 22]. In general, these dyes exhibit structured absorption and fluorescence spectra with mirror-image symmetry and high fluorescence quantum yields. The energy E_{0-0} of the lowest excited singlet state of the di(glycyl)imide dye can be estimated as 2.3 eV from the cross-over point between the excitation and emission spectra (Fig. 3).

The absorption spectra of the di(glycyl)imide dye indicate that the monomer and dimer coexist in H_2O (10^{-3} M NaOH) with an equilibrium constant $K = (1.03 \pm 0.03) \times 10^7$ M^{-1} (24 °C). These is no evidence for higher aggregates until greater than 95% of the dye is present as the dimer. In contrast, the monomer–dimer equilibria of dyes are often complicated by higher aggregates at relatively low degrees of dimerization [50, 59, 61, 64]. Representative values of K for some of the more commonly studied dyes are collected in Table 2. The range of values spans about seven orders of magnitude (10^1 - 10^8 M^{-1}). The value of K for the di(glycyl)imide dye is relatively large, being of the order of the values typically found for water-soluble porphyrins [27, 43, 46, 49, 60, 64] and phthalocyanines [34, 40]. The dissociating effect of EtOH and the aggregating effect of NaCl on the dimer of

TABLE 2

Equilibrium constants K for the dimerization of some common dyes in aqueous solutions

Dye (type)	Conditions[a]	K (M^{-1})	Reference
Fluorescein (xanthene)	20 °C, 0.01 M KCl, pH 12 (NH_4OH)	5	[51]
Orange II[b] (azo)	25 °C	710	[50]
Rhodamine B (xanthene)	20 °C, 0.01 M NaOH (pH 12)	2100	[52]
Thionine[c] (thiazine)	25 °C	4000	[61]
Acridine orange[c] (acridine)	25 °C	1.05×10^4	[37]
3,3'-Diethylthia-carbocyanine[d] (cyanine)	22 °C	2.9×10^4	[36]
Hematoporphyrin (porphyrin)	25 °C, 0.02 M NaOH	1.7×10^5	[49]
H_2TSPC[b] (phthalocyanine)	23 °C	7.6×10^7	[34]

[a]The solvent was H_2O, without added salts unless otherwise indicated.
[b]Sodium salt.
[c]HCl salt.
[d]p-Toluenesulfonate salt.
[e]H_2TSPC is metal-free phthalocyaninetetrasulfonate (sodium salt).

the di(glycyl)imide dye are generally observed in other dye systems as well [32, 37, 41, 42, 45, 46, 48, 54]. The mechanism of dissociation by organic solvents such as EtOH is not well understood, but it probably involves specific dye–solvent interactions rather than being a bulk solvent effect [48]. The effect of NaCl can be attributed to the effect of the salt ions on the structure of water and/or to counterion shielding of the electrostatic repulsion between the negatively charged dye molecules [59].

The rather drastic changes in the absorption and fluorescence properties of the di(glycyl)imide dye that are associated with its dimerization can be interpreted in terms of the molecular exciton theory for plane-parallel (sandwich) dimers in the strong interaction limit (see refs. 36, 39, 41, 44 and 62 and references cited therein). Accordingly, interaction between the transition dipole moments of the two units in the dimer causes a splitting of the S_1 excited state of the monomer into two states, one at a higher energy (transition dipoles in phase) and the other at a lower energy (out of phase) relative to that of the monomer. The appearance of new bands in the absorption spectrum of the dimer (Fig. 5) indicates that the strong interaction limit is applicable [36, 39, 62]. Under this condition, the theory predicts that the absorption bands corresponding to the two dimer transitions have a vibronic structure similar to that of the monomer [36, 62, 63]. The spectrum of the dimer of the di(glycyl)imide dye (Fig. 5) is consistent with this overall description, with the 0–0 transitions of the upper and lower energy S_1 states being near $20\,000$ cm^{-1} and $18\,450$ cm^{-1} respectively. If the transition dipoles of the two dye molecules in the dimer were oriented strictly parallel to each other and perpendicular to the intermolecular axis, only the transition to the upper state of the dimer would be allowed. The fact that transitions to both the upper and lower excited states are allowed indicates that $\pi/2 > \theta > 0$, where θ is the mean angle between the transition dipoles of the dimer units [36, 39]. The polarization axis of this transition is nearly coincident with the molecular long axis of perylene dyes similar to the di(glycyl)imide derivative [70]. The mechanism by which the fluorescence of the di(glycyl)imide dye is quenched upon dimerization most likely involves either enhancement in the rate of intersystem crossing owing to a shifting of the relative energies of the excited singlet and triplet states or enhancement in the rate of internal conversion to the ground state owing to the exciton (dipole–dipole) interaction [36, 39, 53, 57, 62]. The dimers of some dyes are luminescent, especially at low temperatures [41, 47, 53, 55, 56]. In the case of covalently linked porphyrin dimers, the radiationless processes that are responsible for fluorescence quenching appear to require large amplitude fluctuations in the dimer conformation [53]. The emission behavior of the di(glycyl)imide dye falls into this pattern, since the aggregates are fluorescent in frozen lithium acetate glass but not in fluid solution.

The high value of K for dimerization of the di(glycyl)imide dye made it possible to determine the concentration dependence of the fluorescence quantum yield in H_2O (10^{-3} M NaOH) under optically dilute conditions, thus avoiding the necessity for correction factors that are subject to many

approximations [71]. Also, fluorescence self-quenching can be ignored. Although the quantum yield data conformed to eqn. (4), the value of n (1.68) was not an integer (Fig. 6). In their analysis of the absorption spectra of cyanine dyes, Sheppard and Geddes [33] found non-integral values of n, which they attributed to activity factors. The effects of activity coefficients cannot account for the results with the di(glycyl)imide dye, however, because the discrepancies occurred even when the same experimental conditions were used for the absorption ($n = 2.00$) and the quantum yield ($n = 1.68$) measurements. One approach to reconciling the discrepancy between the absorption and the quantum yield results is to assume that a dimer with $0 < \Phi_F < 1$, whose spectral properties resemble those of the monomer, exists as a precursor to the spectroscopically distinguishable dimer. For example, the precursor could have an "open" structure which is stabilized by hydrogen bonding between the dye molecules, which subsequently closes to the plane-parallel (sandwich) conformation. The precursor would have to be more stable than the encounter complex between monomers that is usually included in kinetic schemes for dimer formation [48, 58]. Making the usual steady state approximations, the values of Φ_F would be less than expected from the simple dimer model and the apparent order of the dependence of Φ_F on concentration would be less than 2, as was observed, if such an intermediate existed. However, in contrast to the observations, this model predicts that the log–log plot according to eqn. (4) should be non-linear, and the magnitude of the effect on Φ_F should be significantly less than is observed when reasonable values are chosen for the various kinetic parameters. Thus, the source of the discrepancy between the absorption and the quantum yield results is not yet apparent.

5. Conclusions

The di(glycyl)imide dye (Fig. 1) has a strong tendency to dimerize in water. The monomer–dimer equilibrium is well behaved inasmuch as the law of mass action (eqn. (1)) is obeyed until at least 95% of the dye is dimerized. The non-fluorescent nature of the dimer makes it unlikely that the dye will be useful as a photosensitizer in this state. Fortunately, the dimer can be dissociated by detergent micelles and lipid bilayer vesicles, so that it should be possible to use this dye as a photosensitizer in such media. In fact, the large changes in the spectral properties of the dye that accompany dissociation of the dimer provide a sensitive probe of dye–micelle and dye–vesicle interactions, which are presently being investigated.

Acknowledgments

References

1 T. Maki and H. Hashimoto, *Bull. Chem. Soc. Jpn.*, *25* (1952) 411.
2 T. Maki and H. Hashimoto, *Bull. Chem. Soc. Jpn.*, *27* (1954) 602.
3 K. Venkataraman, *The Chemistry of Synthetic Dyes*, Vol. 2, Academic Press, New York, 1952, pp. 1188 - 1194.
4 A. Rademacher, S. Märkle and H. Langhals, *Chem. Ber.*, *115* (1982) 2927.
5 I. Lukáč and H. Langhals, *Chem. Ber.*, *116* (1983) 3524.
6 H. Langhals, *Chem. Ber.*, *118* (1985) 4641.
7 C. Aubert, J. Fünfschilling, I. Zschokke-Gränacher and H. Langhals, *Fresenius Z. Anal. Chem.*, *320* (1985) 361.
8 R. Raue, H. Harnisch and K. H. Drexhage, *Heterocycles*, *21* (1984) 167.
9 V. Balzani, F. Bolletta, F. Scandola and R. Ballardini, *Pure Appl. Chem.*, *51* (1979) 299.
10 J. R. Darwent, P. Douglas, A. Harriman, G. Porter and M.-C. Richoux, *Coord. Chem. Rev.*, *44* (1982) 83.
11 K. Kalyanasundaram and M. Neumann-Spallart, *J. Phys. Chem.*, *86* (1982) 5163.
12 E. M. Kober, J. L. Marshall, W. J. Dressick, B. P. Sullivan, J. V. Caspar and T. J. Meyer, *Inorg. Chem.*, *24* (1985) 2755.
13 K. Kalyanasundaram, *Chem. Soc. Rev.*, *7* (1978) 453.
14 N. J. Turro, M. Grätzel and A. M. Braun, *Angew. Chem., Int. Ed. Engl.*, *19* (1980) 675.
15 J. K. Hurley and G. Tollin, *Sol. Energy*, *28* (1982) 187.
16 J. J. Fendler, *Membrane Mimetic Chemistry*, Wiley, New York, 1982, pp. 410 - 505.
17 M. Calvin, *Photochem. Photobiol.*, *37* (1983) 349.
18 J. K. Thomas, The chemistry of excitation at interfaces, *ACS Monogr.*, *181* (1984) 1 - 8, 149 - 288.
19 J.-H. Fuhrhop and T. Lehmann, in G. Bauer and H. Sund (eds.), *Optical Properties and Structures of Tetrapyrroles*, de Gruyker, Berlin, 1985, pp. 19 - 39.
20 T. Matsuo, *J. Photochem.*, *29* (1985) 41.
21 J. H. Fendler, *J. Phys. Chem.*, *89* (1985) 2730.
22 W. E. Ford, *J. Photochem.*, *34* (1986) 43.
23 C. Tanford, *The Hydrophobic Effect*, Wiley-Interscience, New York, 1980.
24 J. R. Darwent, *J. Chem. Soc., Chem. Commun.*, (1980) 805.
25 J. K. Hurst, L. Y. C. Lee and M. Grätzel, *J. Am. Chem. Soc.*, *105* (1983) 7048.
26 E. Reddi, G. Jori, M. A. J. Rogers and J. D. Spikes, *Photochem. Photobiol.*, *38* (1983) 639.
27 R. Margalit and S. Cohen, *Biochim. Biophys. Acta*, *736* (1983) 163.
28 D. Kessel, *Photochem. Photobiol.*, *39* (1984) 851.
29 A. Blum and L. I. Grossweiner, *Photochem. Photobiol.*, *41* (1985) 27.
30 M. E. Diaz Garcia and A. Sanz-Medel, *Talanta*, *33* (1986) 255.
31 G. Scheibe, *Kolloid Z.*, *82* (1938) 1.
32 E. Rabinowitch and L. F. Epstein, *J. Am. Chem. Soc.*, *63* (1941) 69.
33 S. E. Sheppard and A. L. Geddes, *J. Am. Chem. Soc.*, *66* (1944) 2003.
34 K. Bernauer and S. Fallab, *Helv. Chim. Acta*, *45* (1962) 2487.
35 K. Bergman and C. T. O'Konski, *J. Phys. Chem.*, *67* (1963) 2169.
36 M. Kasha, H. R. Rawls and M. Ashraf El-Bayoumi, *Pure Appl. Chem.*, *11* (1965) 371.
37 W. West and S. Pearce, *J. Phys. Chem.*, *69* (1965) 1894.
38 M. E. Lamm and D. M. Neville, Jr., *J. Phys. Chem.*, *69* (1965) 3872.
39 R. S. Becker, *Theory and Interpretation of Fluorescence and Phosphorescence*, Wiley-Interscience, New York, 1969, pp. 234 - 238.
40 H. Sigel, P. Waldmeier and B. Prijs, *J. Inorg. Nucl. Chem.*, *7* (1971) 161.
41 R. W. Chambers, T. Kajiwara and D. R. Kearns, *J. Phys. Chem.*, *78* (1974) 380.
42 D. G. Doff and C. H. Giles, in F. Franks (ed.), *Water, a Comprehensive Treatise*, Vol. 4, Plenum, New York, 1975, p. 169.

43 M. Krishnamurthy, J. R. Sutter and P. Hambright, *J. Chem. Soc., Chem. Commun.*, (1975) 13.
44 V. J. Koéster and F. K. Fong, *J. Phys. Chem.*, *80* (1976) 2310.
45 A. H. Herz, *Adv. Colloid Interface Sci.*, *8* (1977) 237.
46 W. I. White, in D. Dolphin (ed.), *The Porphyrins*, Vol. 5, Academic Press, New York, 1978, p. 303.
47 J. Knof, F.-J. Theiss and J. Weber, *Z. Naturforsch., Teil A*, *33* (1978) 98.
48 T. G. Dewey, P. S. Wilson and D. H. Turner, *J. Am. Chem. Soc.*, *100* (1978) 4550.
49 G. A. Karns, W. A. Gallagher and W. B. Elliot, *Bioorg. Chem.*, *8* (1979) 69.
50 R. L. Reeves, M. S. Maggio and S. A. Harkaway, *J. Phys. Chem.*, *83* (1979) 2359.
51 I. López Arbeloa, *J. Chem. Soc., Faraday Trans. II*, *77* (1981) 1725.
52 I. López Arbeloa and P. Ruiz Ojeda, *Chem. Phys. Lett.*, *87* (1982) 556.
53 R. R. Bucks, T. L. Netzel, I. Fujita and S. G. Boxer, *J. Phys. Chem.*, *86* (1982) 1947.
54 V. Vitagliano, in E. Wyn-Jones and J. Gormally (eds.), *Aggregation Processes in Solution*, Elsevier, Amsterdam, 1983, p. 271.
55 I. López Arbeloa, *Dyes Pigm.*, *4* (1983) 213.
56 M. Septinus, W. Seiffert and H. W. Zimmermann, *Histochem.*, *79* (1983) 443.
57 F. G. Patterson, H. W. Lee, W. L. Wilson and M D. Fayer, *Chem. Phys.*, *84* (1984) 51.
58 W. Ohling, *Ber. Bunsenges. Phys. Chem.*, *88* (1984) 109.
59 E. H. Braswell, *J. Phys. Chem.*, *88* (1984) 3653.
60 J. A. Shelnutt, M. M. Dobry and J. D. Satterlee, *J. Phys. Chem.*, *88* (1984) 4980.
61 W. C. Lai, N. S. Dixit and R. A. Mackay, *J. Phys. Chem.*, *88* (1984) 5364.
62 V. Sundström and T. Gillbro, *J. Chem. Phys.*, *83* (1985) 2733.
63 D. Fornasiero and T. Kurusev, *J. Chem. Soc., Faraday Trans. II*, *82* (1986) 15.
64 A. Corsini and O. Herrmann, *Talanta*, *33* (1986) 335.
65 C. Sandorfy, *Electronic Spectra and Quantum Chemistry*, Prentice–Hall, Englewood Cliffs, NJ, 1964, pp. 90 - 109.
66 J. V. Morris, M. A. Mahaney and J. R. Huber, *J. Phys. Chem.*, *80* (1976) 969.
67 J. B. Birks, *Photophysics of Aromatic Molecules*, Wiley-Interscience, London, 1970, pp. 51 - 52, 184.
68 S. Hirayama and D. Phillips, *J. Photochem.*, *12* (1980) 139.
69 R. F. Kubin and A. N. Fletcher, *J. Lumin.*, *27* (1982) 455.
70 T. M. Leslie, J. W. Goodby and R. W. Filas, in A. C. Griffin and J. E. Johnson (eds.), *Liquid Crystals and Ordered Fluids*, Vol. 4, Plenum, New York, 1984, p. 43.
71 I. López Arbeloa, *J. Photochem.*, *14* (1980) 97.